Lanthanide Complexes with an Azo-dye Chromophore Ligand: Syntheses, Crystal Structures, and Near-infrared Luminescence by Long-wavelength Excitation

Yun-long Chen[a,b], Min Feng[b,c*], Xiaofei Zhu[a*], Zhiping Zheng[b,c*]

a School of Chemistry and Life Science, Changchun University of Technology, Changchun, 130012, China

b Department of Chemistry, Southern University of Science and Technology, Shenzhen, 518055, China

c Key University Laboratory of Rare Earth Chemistry of Guangdong, Southern University of Science and Technology, Shenzhen, Guangdong 518055.

E-mail addresses: fengm@sustech.edu.cn (M. Feng), zhuxiaofei@ccut.edu.cn (X. Zhu), zhengzp@sustech.edu.cn (Z. Zheng)

Contents

Table S1. X-ray Crystallographic Data for **1**-**3**.

complex	1	2	3
Empirical formula	$C_{32}H_{54}Yb_2N_4O_{34}S_4$	$C_{32}H_{54}Er_2N_4O_{34}S_4$	$C_{32}H_{54}Gd_2N_4O_{34}S_4$
Formula weight	1513.11	1501.55	1481.53
Temperature/K	100.02	100.05	99.99
Crystal system	monoclinic	monoclinic	monoclinic
Space group	$P2_1/n$	$P2_1/n$	$P2_1/n$
a/Å	15.1083(9)	15.1450(6)	15.2177(10)
b/Å	7.4003(5)	7.4186(3)	7.4551(4)
c/Å	23.3340(14)	23.3610(8)	23.3788(13)
α/°	90	90	90
β/°	107.382(3)	107.3690(10)	107.394(2)
γ/°	90	90	90
Volume/Å^3	2489.7(3)	2505.04(17)	2531.0(3)
Z	2	2	2
ρ_{calc}g/cm^3	2.018	1.991	1.944
μ/mm^{-1}	4.009	3.602	2.869
F(000)	1500	1492	1476
Radiation	Mo*K*α (λ = 0.71073)	Mo*K*α (λ = 0.71073)	Mo*K*α (λ = 0.71073)
Reflections collected	25613	30812	20817
Independent reflections	6421 [R_{int} = 0.0953, R_{sigma} = 0.0920]	5775 [R_{int} = 0.0638, R_{sigma} = 0.0452]	5213 [R_{int} = 0.0747, R_{sigma} = 0.0665]
Data/restraints/ parameters	6421/1/360	5775/0/360	5213/1/360
Goodness-of-fit on F^2	1.007	1.04	1.042
Final R indexes [I>=2σ(I)]	R_1 = 0.0455, wR_2 = 0.0794	R_1 = 0.0301, wR_2 = 0.0663	R_1 = 0.0395, wR_2 = 0.0864
Final R indexes [all data]	R_1 = 0.0850, wR_2 = 0.0936	R_1 = 0.0301, wR_2 = 0.0663	R_1 = 0.0538, wR_2 = 0.0929
Largest diff. peak/hole / eÅ^{-3}	1.25/-1.55	1.19/-1.16	1.34/-1.06
CCDC number	2303845	2303847	2303852

Table S2. X-ray Crystallographic Data for **4**-**6**.

complex	4	5	6
Empirical formula	$C_{52}H_{90}Yb_2N_4O_{28}S_{16}$	$C_{52}H_{90}Er_2N_4O_{28}S_{16}$	$C_{52}H_{90}Gd_2N_4O_{28}S_{16}$
Formula weight	2126.35	2114.79	2094.77
Temperature/K	100	100	100.02
Crystal system	triclinic	triclinic	triclinic
Space group	*P*-1	*P*-1	*P*-1
a/Å	11.2546(8)	11.2494(6)	11.2789(8)
b/Å	14.4042(9)	14.5051(7)	14.5397(11)
c/Å	15.0132(9)	15.0460(8)	15.0454(11)
α/°	113.027(3)	113.056(3)	113.012(3)
β/°	90.449(4)	90.302(3)	90.218(3)
γ/°	111.806(4)	111.853(3)	111.884(2)
Volume/Å^3	2046.0(2)	2063.62(19)	2074.8(3)
Z	1	1	1
ρ_{calc}g/cm^3	1.726	1.702	1.677
μ/mm^{-1}	10.4	9.526	2.063
F(000)	1074	1070	1062
Radiation	Ga*K*α (λ = 1.34139)	Ga*K*α (λ = 1.34139)	Mo*K*α (λ = 0.71073)
Reflections collected	51458	24195	26624
Independent reflections	9428 [R_{int} = 0.0857, R_{sigma} = 0.0624]	7841 [R_{int} = 0.0747, R_{sigma} = 0.0895]	9543 [R_{int} = 0.0622, R_{sigma} = 0.0755]
Data/restraints/parameters	9428/0/452	7841/0/452	9543/0/452
Goodness-of-fit on F^2	1.105	1.064	1.016
Final R indexes [I>=2σ (I)]	R_1 = 0.0425, wR_2 = 0.1046	R_1 = 0.0504, wR_2 = 0.1158	R_1 = 0.0393, wR_2 = 0.0772
Final R indexes [all data]	R_1 = 0.0533, wR_2 = 0.1078	R_1 = 0.0668, wR_2 = 0.1211	R_1 = 0.0572, wR_2 = 0.0824
Largest diff. peak/hole / e Å^{-3}	0.79/-1.53	0.78/-1.41	1.81/-0.96
CCDC number	2303867	23038468	2303869

Table S3. Selected bonds lengths [Å] for **1**-**3**.

	1	2	3
Atom	Length	Length	Length
Ln1-O1	2.242(4)	2.269(3)	2.313(3)
Ln1-O2	2.207(4)	2.232(3)	2.274(3)
Ln1-O4^1	2.427(4)	2.426(3)	2.454(3)
Ln1-O1W	2.337(4)	2.362(3)	2.416(4)
Ln1-O2W	2.302(4)	2.320(3)	2.367(4)
Ln1-O3W	2.397(4)	2.417(3)	2.459(3)
Ln1-O4W	2.293(4)	2.320(3)	2.377(4)
Ln1-O5W	2.393(4)	2.421(3)	2.459(4)

O4^1 is the oxygen on an adjacent ligand (HC2R).

Table S4. Selected bonds lengths [Å] for **4**-**6**.

	4	5	6
Atom	Length	Length	Length
Ln-O1	2.270(3)	2.301(4)	2.353(3)
Ln-O2	2.285(3)	2.318(4)	2.360(3)
Ln-O8^1	2.324(3)	2.352(4)	2.391(3)
Ln-O9	2.279(3)	2.315(4)	2.363(3)
Ln-O10	2.423(3)	2.390(3)	2.467(3)
Ln-O11	2.374(3)	2.434(4)	2.423(3)
Ln-O12	2.269(3)	2.306(4)	2.342(3)
Ln-O13	2.282(3)	2.281(4)	2.352(3)

O8^1 is the oxygen on an adjacent ligand (HC2R).

Table S5. Coordination geometry of complexes **1**-**6**.

Eight-Coordinated Metal centers							
	O_hCU	D_{4d}SAPR	D_{2d}TDD	C_{2v}JBTPR	C_{2v}BTPR	D_{2d}JSD	T_dTT
1	9.735	2.402	0.376	2.337	2.139	2.485	10.438
2	9.82	2.461	0.413	2.422	2.188	2.558	10.525
3	9.799	2.534	0.447	2.56	2.277	2.697	10.546
4	10.213	3.066	0.374	2.75	2.176	2.288	10.838
5	10.161	3.002	0.36	2.804	2.139	2.321	10.803
6	10.058	2.977	0.375	2.877	2.143	2.484	10.754

CU: Cube; SAPR: Square antiprism; TDD: Triangular dodecahedron; JBTPR: Biaugmented trigonal prism J50; BTPR: Biaugmented trigonal prism; JSD: Snub diphenoid J84; TT: Triakis tetrahedron. HPY: Hexagonal pyramid; PBPY: Pentagonal bipyramid; COC: Capped octahedron; CTPR: Capped trigonal prism; JPBPY: Johnson pentagonal bipyramid J13; JETPY: Johnson elongated triangular pyramid J7.

Table S6. TD-DFT calculated excitation energies and main compositions of the low-lying electronic transitions for H_2C2R^{2-}.

Excited state	E (eV)	E (nm)	f	Tansition		Contribution	Assignment	
1	2.5834	480	0.6944	HOMO	→ LUMO	98.70%	π → π*	π→π*
3	3.3932	365	0.3519	HOMO-1	→ LUMO	72.70%	π → π*	
				HOMO-3	→ LUMO	14.80%	π → π*	π→π*
				HOMO-2	→ LUMO	9.50%	π → π*	
4	3.4636	358	0.0348	HOMO-2	→ LUMO	89.60%	n → π*	n→π*
				HOMO-1	→ LUMO	6.40%	π → π*	
8	4.2243	294	0.1751	HOMO	→ LUMO+1	80.30%	π → π*	π→π*
				HOMO-7	→ LUMO	13.70%	π → π*	
10	4.4906	276	0.1389	HOMO-7	→ LUMO	71.40%	π → π*	
				HOMO	→ LUMO+1	9.10%	π → π*	π→π*
				HOMO	→ LUMO+2	6.60%	π → π*	
11	4.5563	272	0.1485	HOMO	→ LUMO+2	76.50%	π → π*	π→π*
				HOMO-7	→ LUMO	5.30%	π → π*	
14	4.788	259	0.1068	HOMO	→ LUMO+3	62.50%	π → π*	
				HOMO-10	→ LUMO	11.70%	π → π*	π→π*
				HOMO	→ LUMO+2	5.00%	π → π*	
23	5.4006	230	0.5475	HOMO-1	→ LUMO+1	49.90%	π → π*	
				HOMO-3	→ LUMO+1	26.10%	π → π*	π→π*
				HOMO	→ LUMO+3	6.80%	π → π*	

Table S7. TD-DFT calculated excitation energies and main compositions of the low-lying electronic transitions for $[Lu_2(HC2R)_2(DMSO)_{10}]$.

Excited state	E (eV)	E (nm)	f	Tansition		Contribution	Assignment		
1	1.4963	829	0.0172	HOMO	→ LUMO	50.70%	n	→ π*	n→π*
				HOMO-1	→ LUMO+1	48.70%	n	→ π*	
5	2.0984	591	0.3951	HOMO-2	→ LUMO	47.40%	π	→ π*	π→π*
				HOMO-3	→ LUMO+1	44.10%	π	→ π*	
11	2.6485	468	0.5621	HOMO-4	→ LUMO	35.20%	π	→ π*	π→π*
				HOMO-5	→ LUMO+1	34.70%	π	→ π*	
				HOMO-6	→ LUMO	11.30%	π, σ	→ π*	
				HOMO-7	→ LUMO+1	9.60%	π, σ	→ π*	
19	3.3305	372	0.0164	HOMO-14	→ LUMO	24.60%	σ, π	→ π*	σ, π→π*
				HOMO-15	→ LUMO+1	22.10%	σ, π	→ π*	
				HOMO-12	→ LUMO	12.80%	π	→ π*	
				HOMO-10	→ LUMO	8.50%	π	→ π*	
				HOMO-19	→ LUMO+1	8.00%	σ, π	→ π*	
				HOMO-11	→ LUMO+1	7.00%	π	→ π*	
21	3.357	369	0.0711	HOMO-10	→ LUMO	41.70%	π	→ π*	π→π*
				HOMO-11	→ LUMO+1	38.10%	π	→ π*	
				HOMO-12	→ LUMO	6.50%	π	→ π*	
34	3.6237	342	0.3428	HOMO-13	→ LUMO+1	39.40%	π	→ π*	π→π*
				HOMO-12	→ LUMO	26.60%	π	→ π*	
				HOMO-14	→ LUMO	16.30%	σ, π	→ π*	

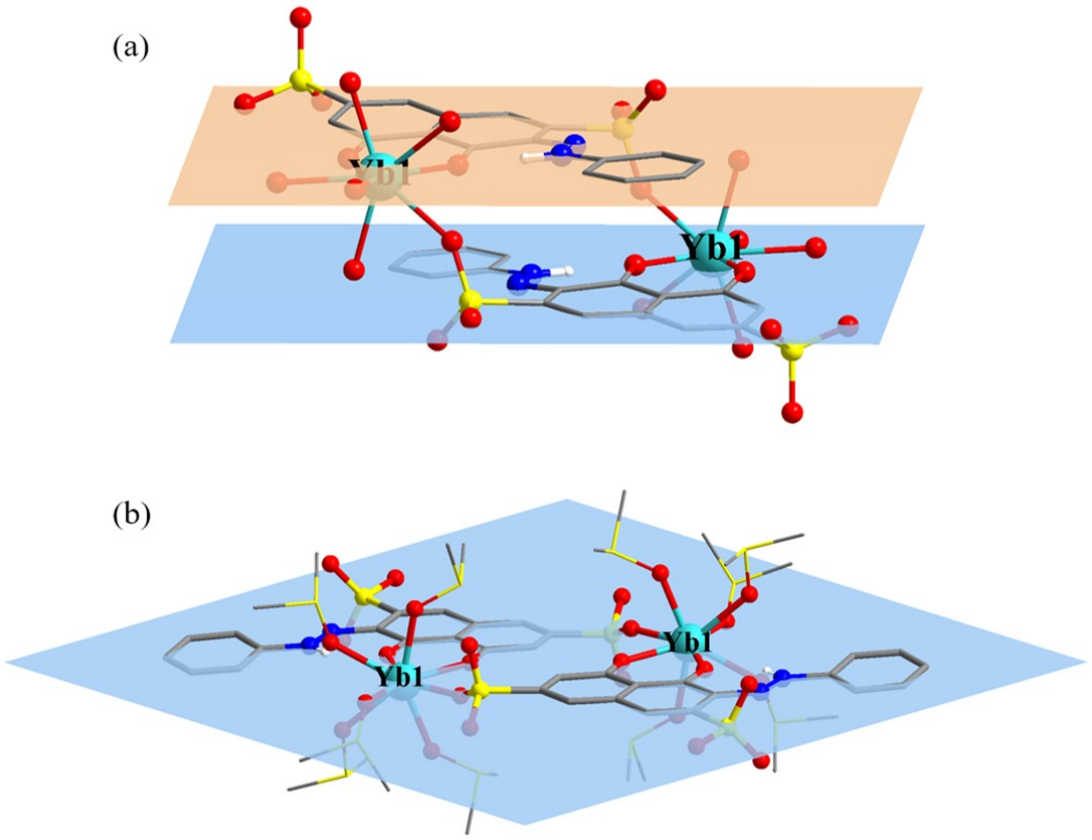

Figure S1. The molecular structures of complexes **1** (a) and **9** (b) with the main planes of their ligands. All H atoms are omitted except the H on N. Color code: Cyan (Er), Red (O), Blue (N), Yellow (S), Gray (C), White (H).

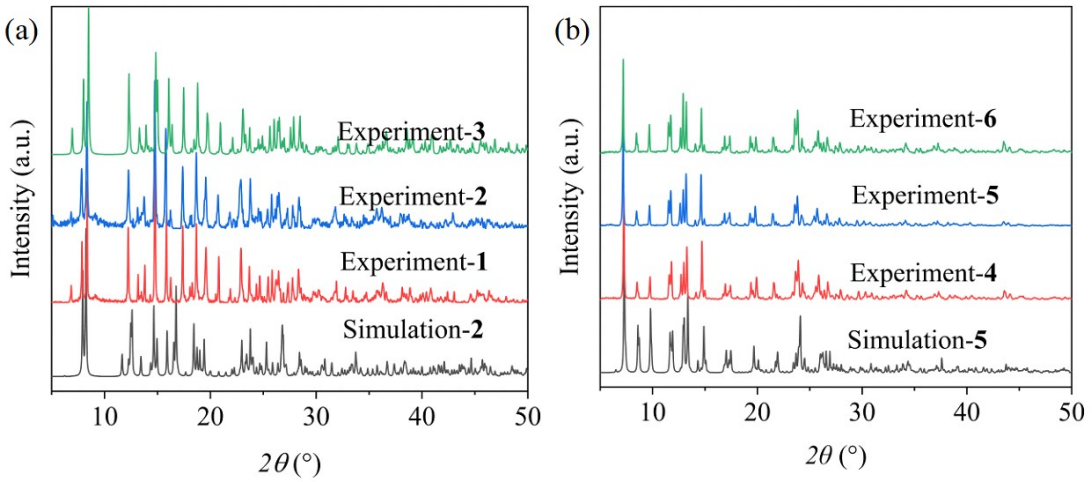

Figure S2. Powder X-ray diffraction patterns of complexes **1**-**3** and **4**-**6** (b).

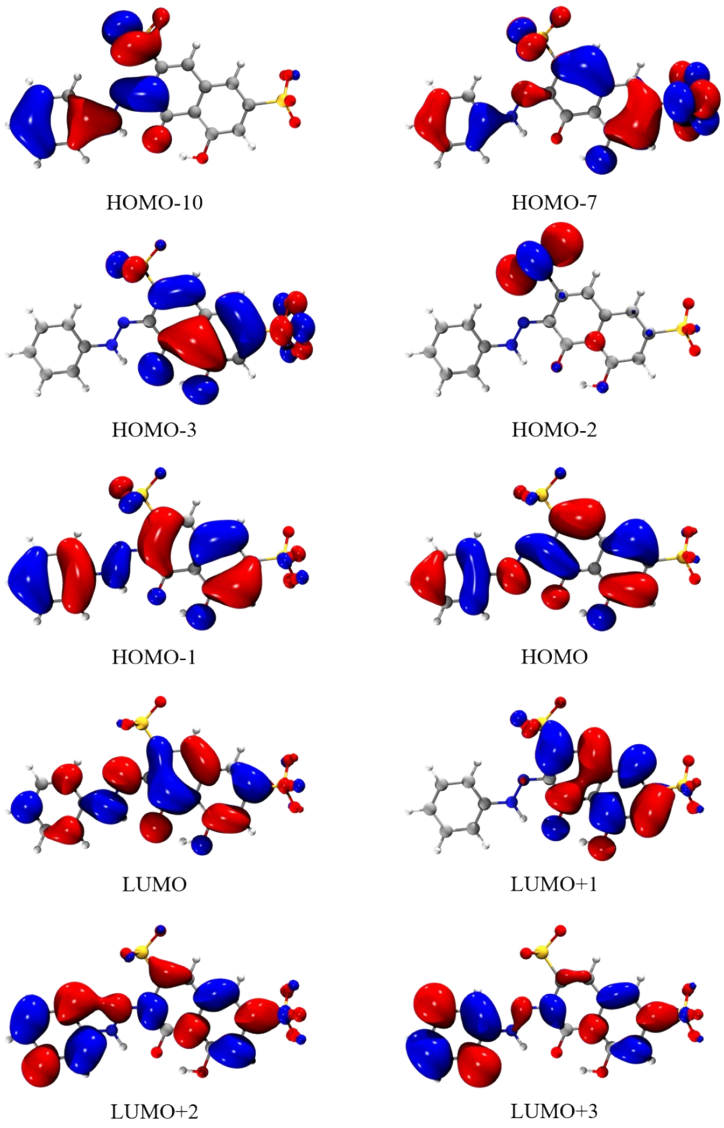

Figure S3. The molecular orbitals of H_2C2R^{2-}.

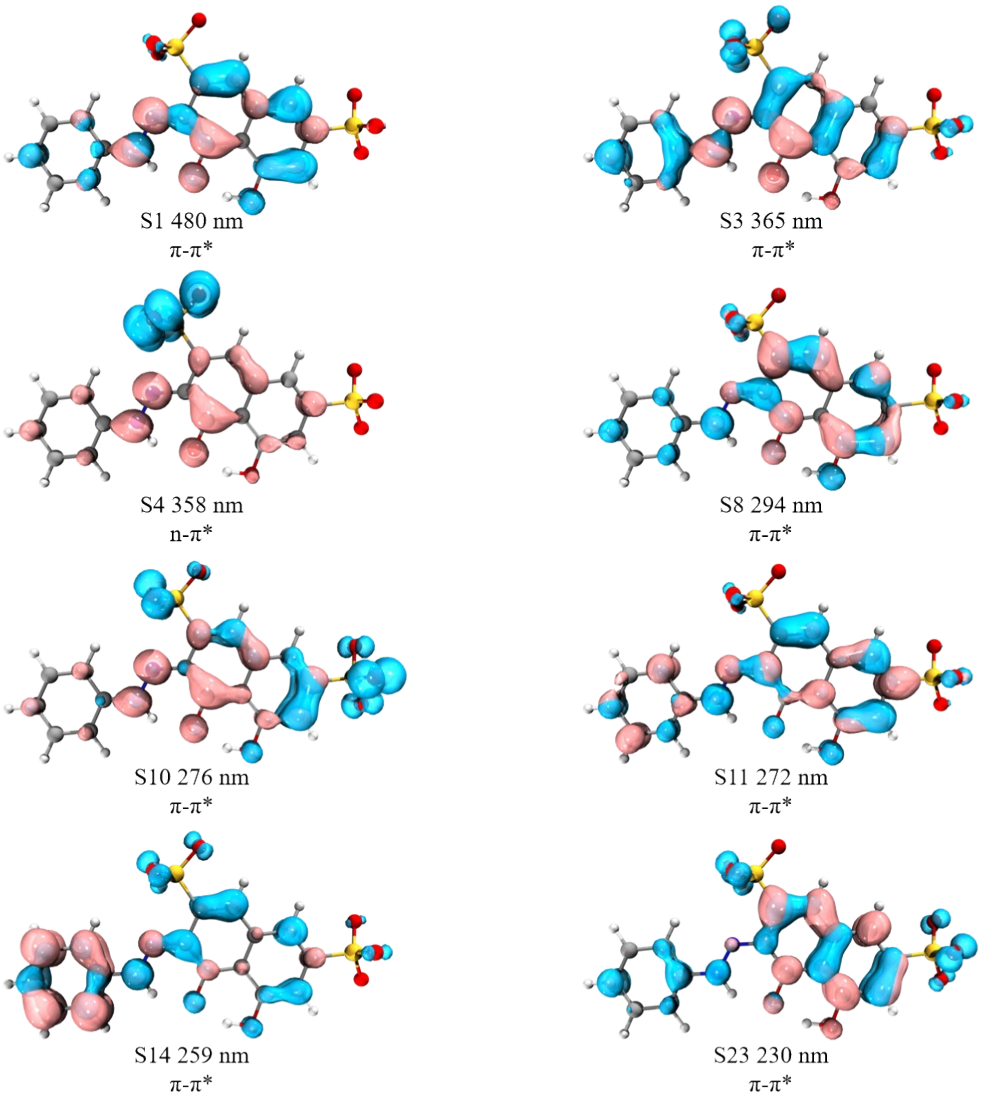

Figure S4. The S1, S3, S4, S8, S10, S11 (f > 0.03) hole and electron distributions of H_2C2R^{2-}. Pink: hole, cyan: electron.

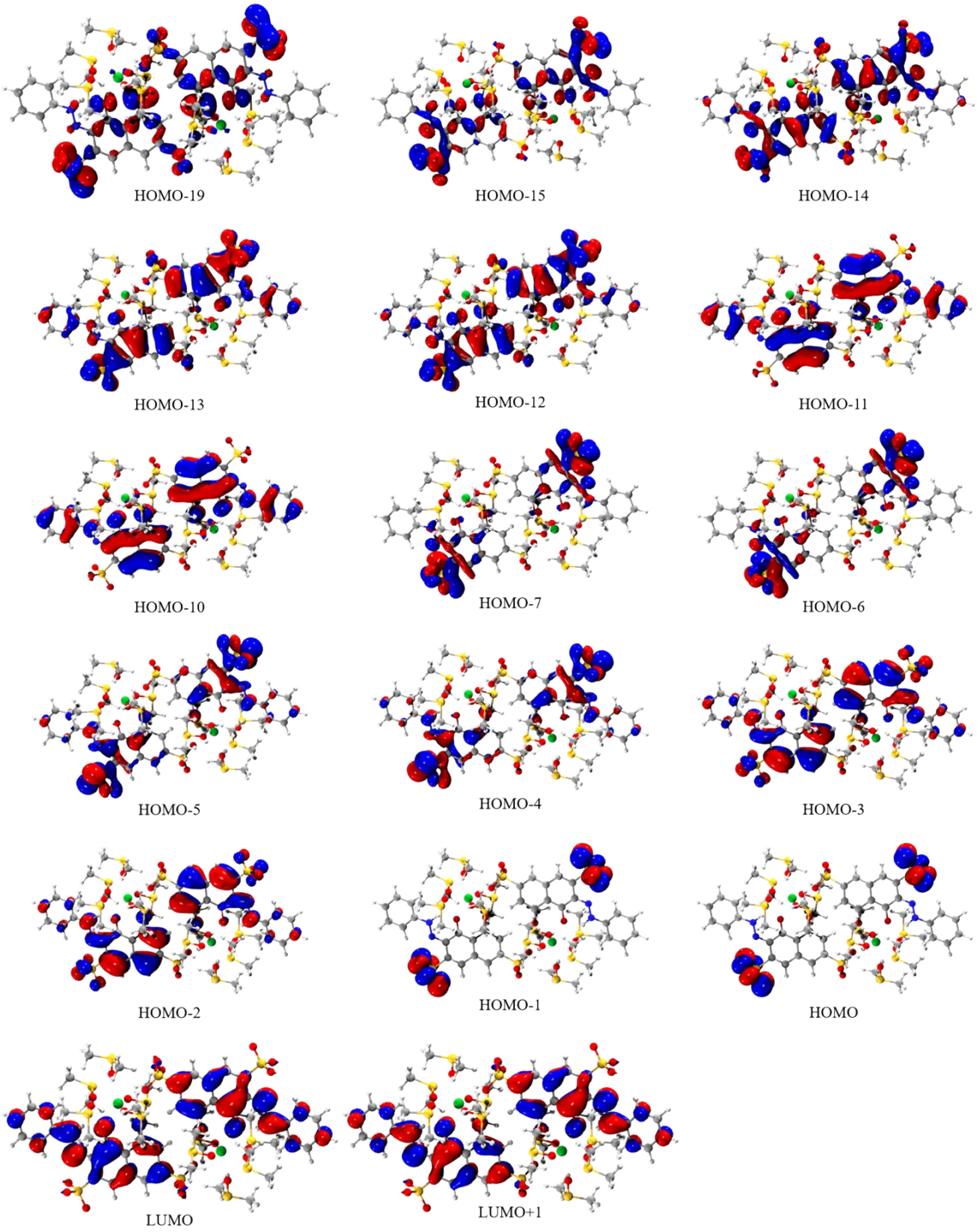

Figure S5. The molecular orbitals of $[Lu_2(HC2R)_2(DMSO)_{10}]$.

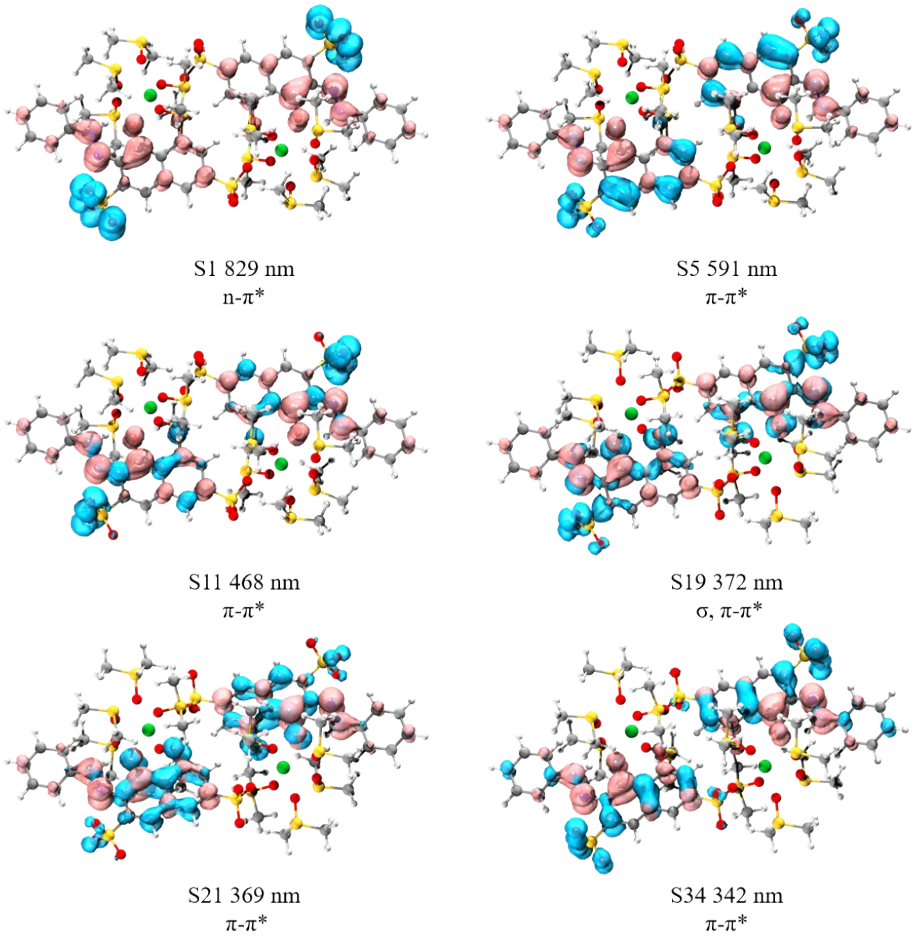

Figure S6. The S1, S5, S11, S19, S21, S34 (f > 0.01) Hole and electron distributions of $[Lu_2(HC2R)_2(DMSO)_{10}]$. Pink: hole, cyan: electron.

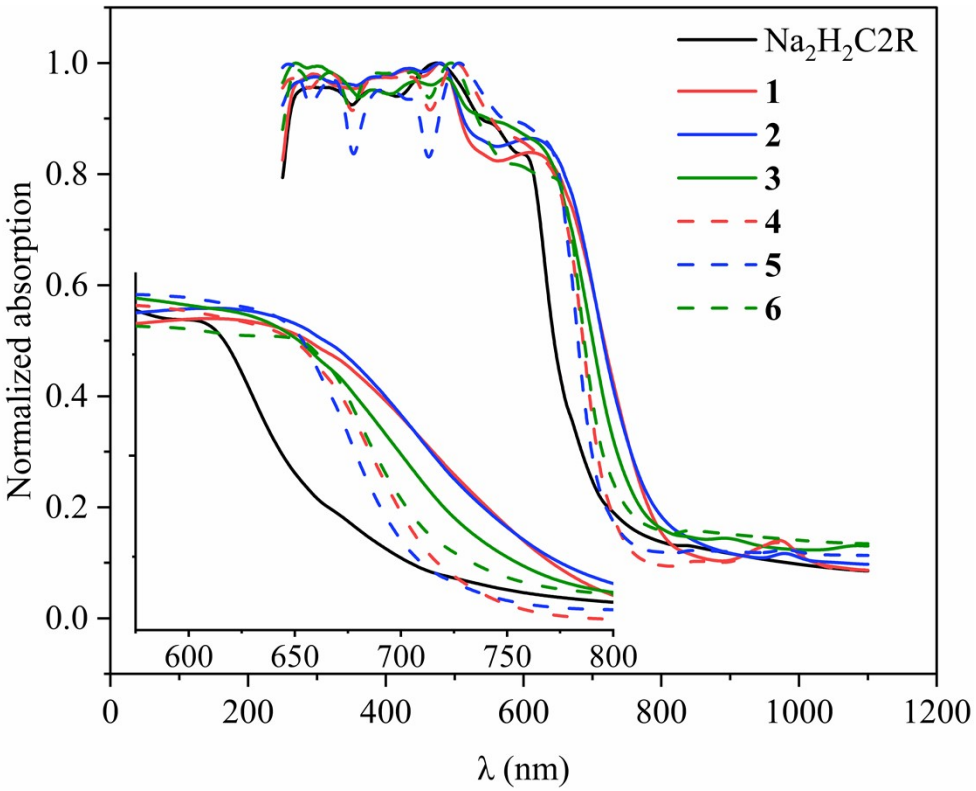

Figure S7. UV-vis absorption spectra of ligand Na_2H_2C2R and complexes **1**-**6** in solid state.

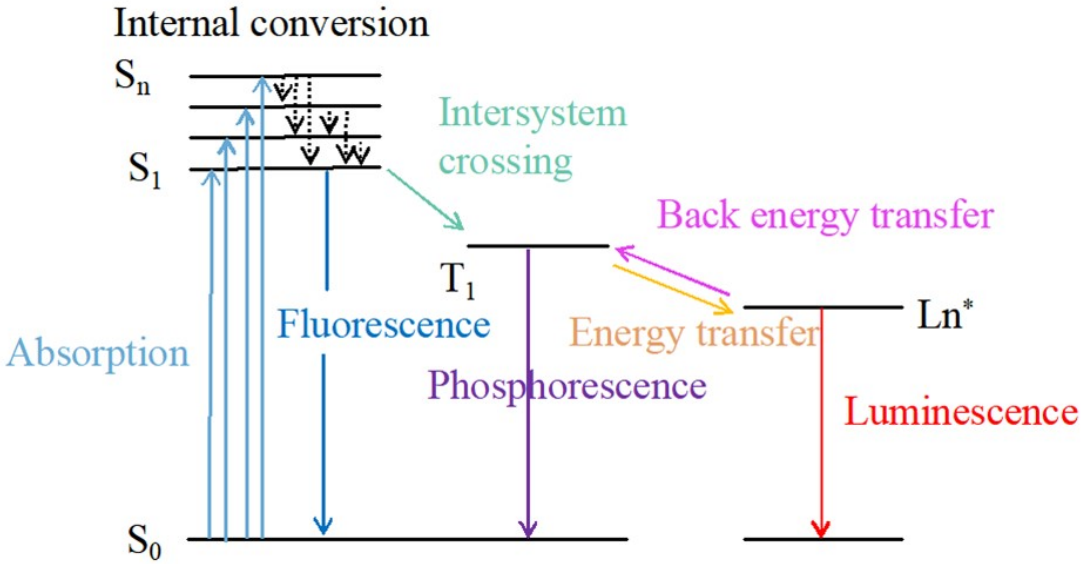

Figure S8. Energy level diagram for Ln complexes sensitized via a ligand-centered triplet excited state.

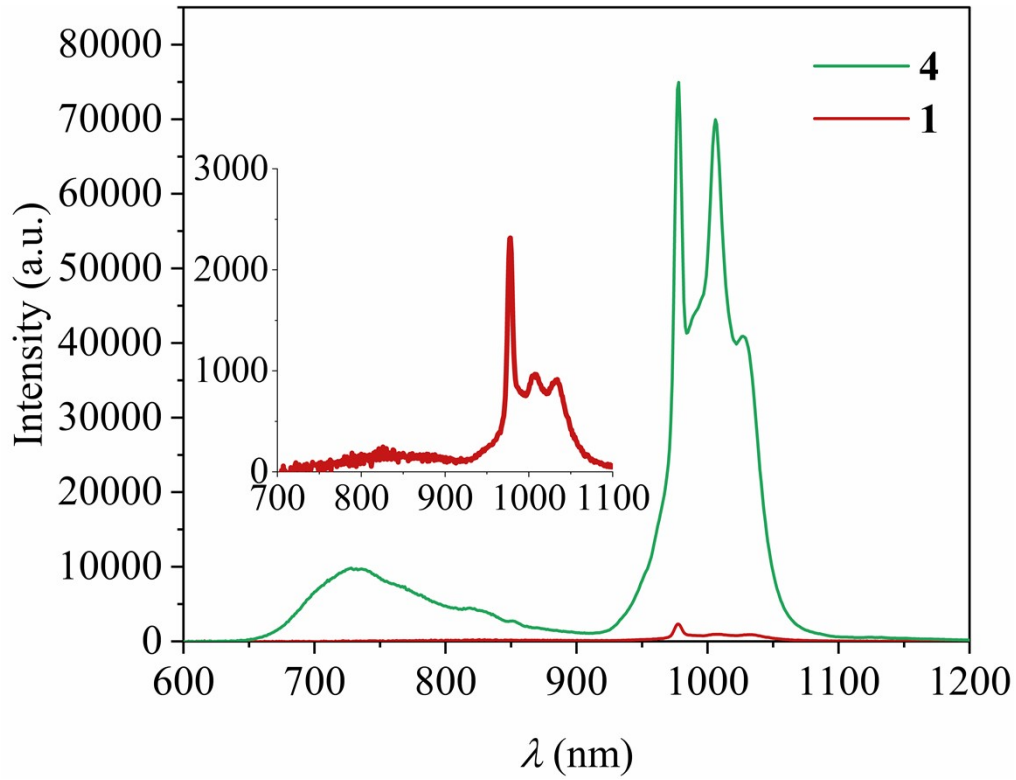

Figure S9. Emission spectra of **1** and **4**.

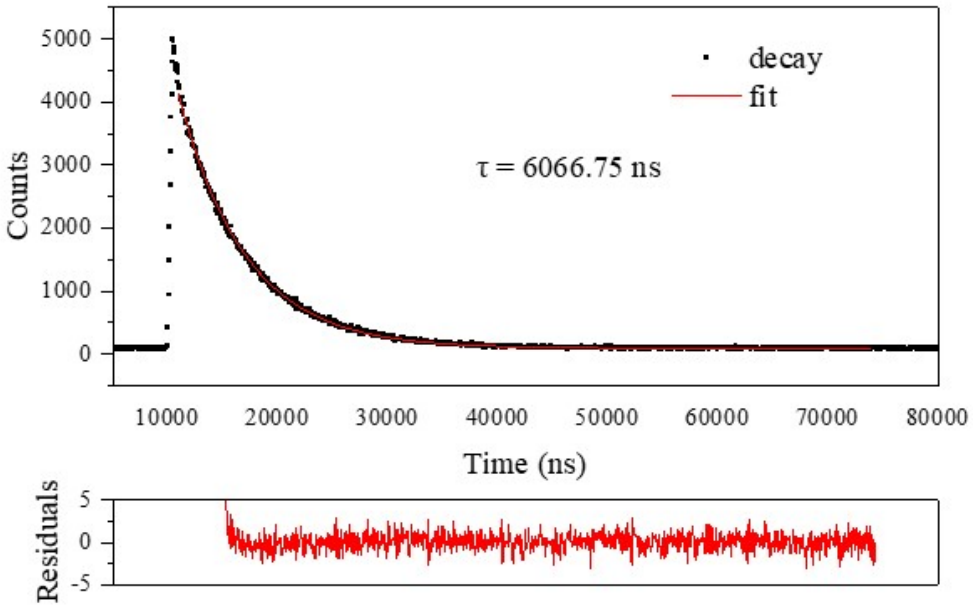

Figure S10. NIR luminescence decay curve of complex **4** at 980 nm.

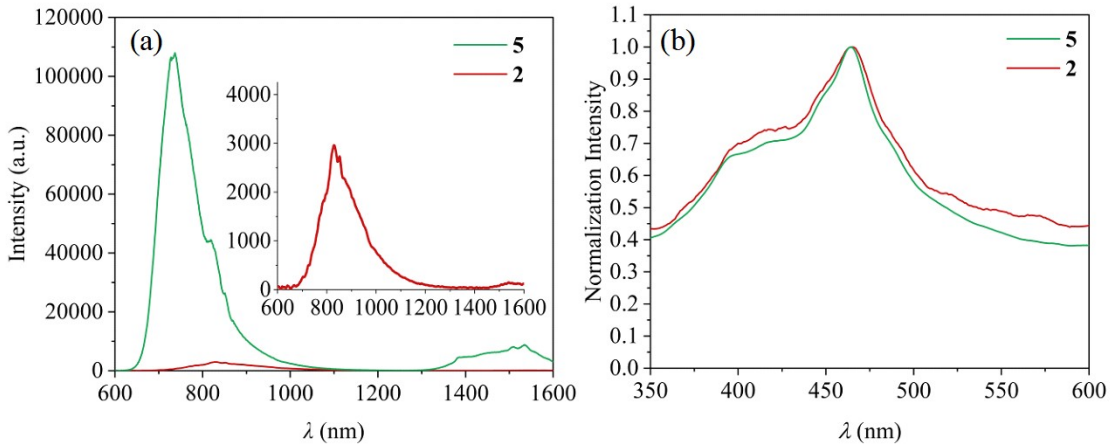

Figure S11. NIR emission (a) and excitation spectra (b) of **2** and **5**.

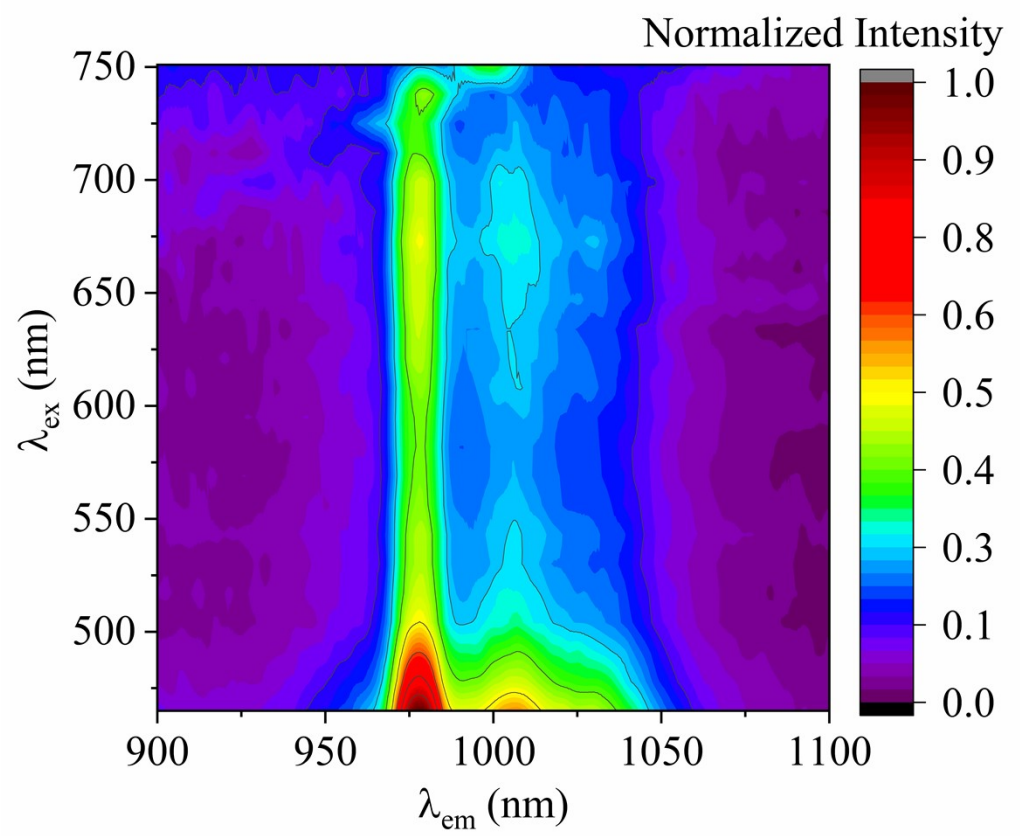

Figure S12. Emission spectra of **1** under λ_{ex} = 465–751 nm.

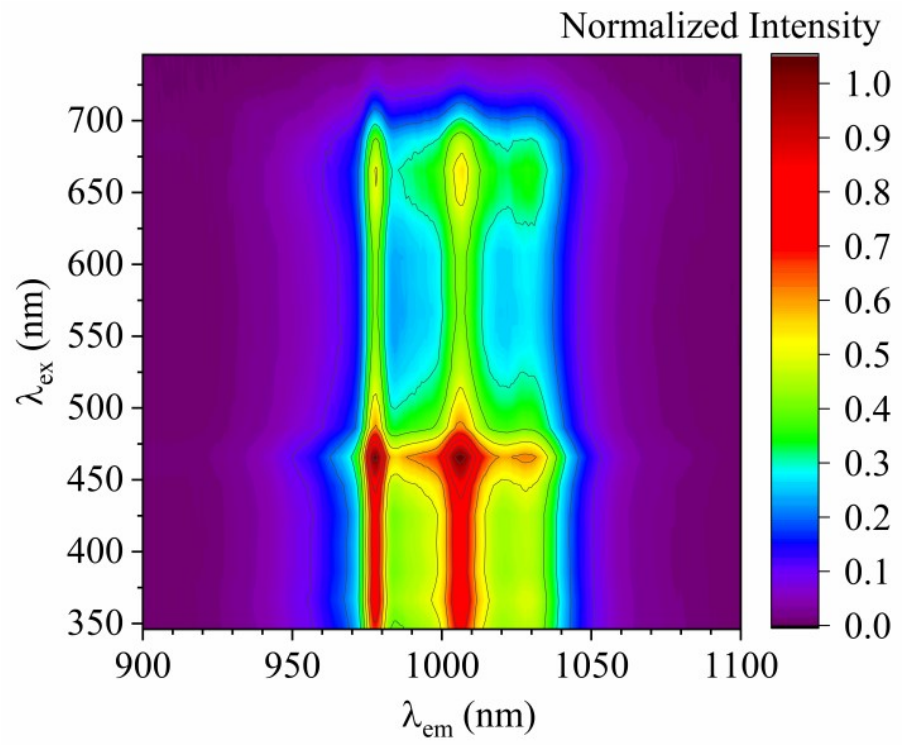

Figure S13. Emission spectra of **1** under λ_{ex} = 346–746 nm.

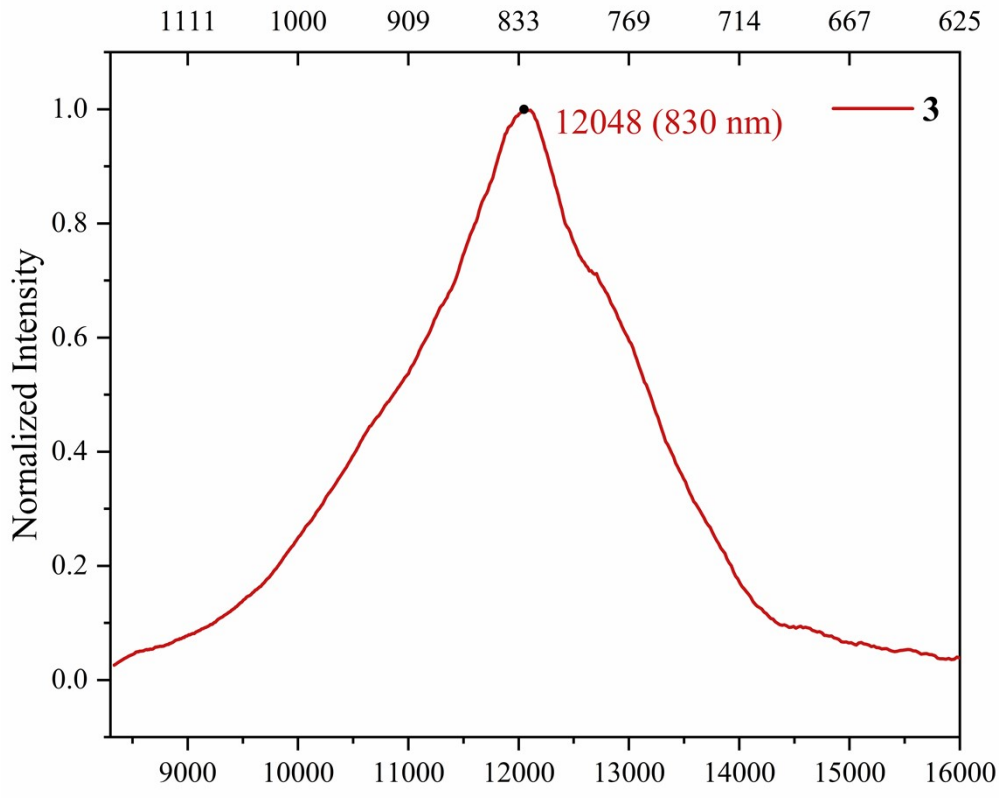

Figure S14. Phosphorescent spectrum of complex **3** at room temperature.

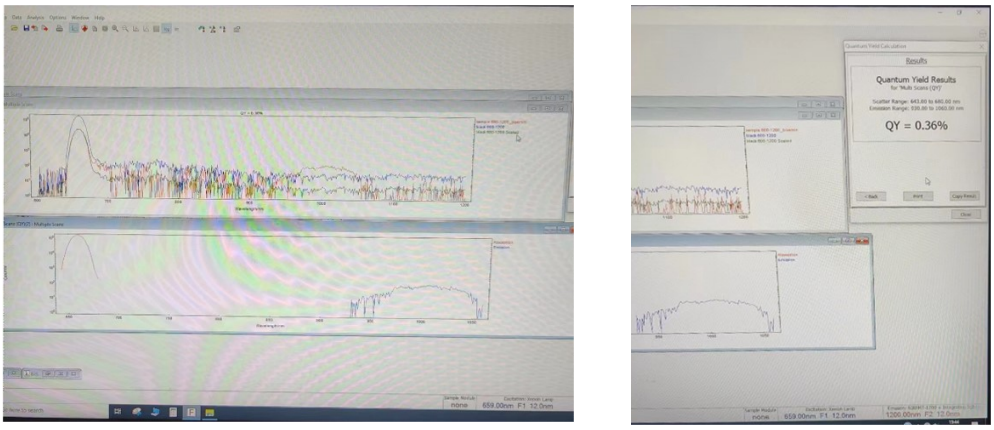

Figure S15. The absolute QY measurement of **4** (λ_{ex} = 659 nm). Results via FLS1000 – Integrating Sphere